

# Application of Data Sensing Enhancement Technology in Trace Detection of C5-PFK Decomposition Gas and Its Engineering Application Prediction

Liangjun Dai, Baojia Deng, Shiling Zhang<sup>\*1</sup>, Long Li

<sup>\*</sup>State Grid Chongqing Electric Power Company Chongqing Electric Power Research Institute, Chongqing, 401123, China

## ABSTRACT

This article applies the structural dimensions of the switchgear, the multi physics analysis is used to establish the internal model of the gas chamber, which mainly includes the main busbar, busbar sleeve, the vacuum arc extinguishing the chamber shell, the internal insulation cone, the three position isolation grounding switch, connection device and other components. The various parameters in the actual C5F100 gas insulated switchgear are distributed parameters, but in practical analysis, the centralized parameter chain network is usually used instead of the actual distributed parameters to construct equivalent circuit of winding under the impulse voltage. Due to the high frequency of impulse voltage and the small ratio of winding resistance to inductive and capacitive reactance, the damping effect of resistance can be ignored in analysis. The sensing system for the H<sub>2</sub>O and HF gas detection was designed using the 1392nm and 1278nm DFB lasers combined with absorption spectroscopy technology. The display host LCD circuit is powered by the 5V power supply, while the general digital circuit is powered by the 3.3V power supply. This system uses the TPS5430 DC-DC buck chip to reduce the voltage to 5V, then uses the LDO chip LM1117-3.3 to reduce the voltage to 3.3V for use in digital system.

**Keywords:** Structural dimension, Switchgear, Multi physics analysis, C5F100 gas insulated

## 1. INTRODUCTION

In recent years, perfluoropentanone(C5F10O) has attracted much attention due to its excellent environmental protection (GWP of about 1) and insulation performance (about twice that of SF<sub>6</sub> gas). Although C5F10O has a high liquefaction temperature (about 26.9°C at one atmosphere), it can achieve sufficient insulation strength when mixed with gases such as CO<sub>2</sub>, N<sub>2</sub>, or air to meet requirements of equipment operating temperature[1-5]. At present, scholars both domestically and internationally have conducted extensive research on the physicochemical properties, the insulation performance, decomposition characteristics, and other related properties of C5F10O gas. Overall, existing studies have confirmed that C5F10O mixed gas has the excellent comprehensive characteristics such as the environmental protection, insulation, and decomposition, and has the potential to replace SF<sub>6</sub> gas in various medium and high voltage gas insulation equipment.

The busbar compartment of switchgear is usually located at the top of the switchgear and is an independent compartment. The branch busbar are fixed on static contact box and overlapped with the main busbar. The main busbar is connected to adjacent cabinets through the busbar wall bushing. If there is the internal fault arc in the busbar room, the through wall sleeve serves as isolation measure, which can limit spread of the accident to adjacent cabinets and ensure the mechanical strength of the busbar which is shown in Figure 1.



Figure 1. Connection between static contact box and branch busbar.

<sup>1</sup> \*526793305@qq.com

The insulation rod is located on the pole of the arc extinguishing chamber, with one end of the embedded part connected to the high potential and the other end connected to the low potential movable pin. Therefore, the insulation rod plays an important insulation role between them and is also structure in switchgear where the electric field is easily concentrated. The high potential may discharge through epoxy resin at the low potential gap. Therefore, this position can be improved by pouring shielding cover at the epoxy resin position of the insulation rod, installing an umbrella skirt on the insulator, and adding an external shielding cover at the port to weaken the nearby electric field and enhance the insulation effect[6].

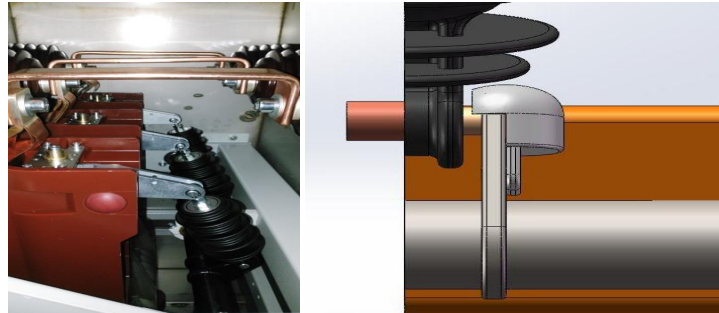


Figure 2. Improvement diagram of insulation rod.

Based on the structural dimensions of the switchgear, the multi physics analysis software is used to establish the internal model of the gas chamber, which mainly includes the main busbar, busbar sleeve, the vacuum arc extinguishing chamber shell[7,8], internal insulation cone, three position isolation grounding switch, connection device and other components shown in Figure 3. Relative permittivity and resistivity are set for each component's composition material(stainless steel, epoxy resin, polyvinyl chloride, copper, etc.) to accurately calculate the electric field distribution inside the gas chamber.

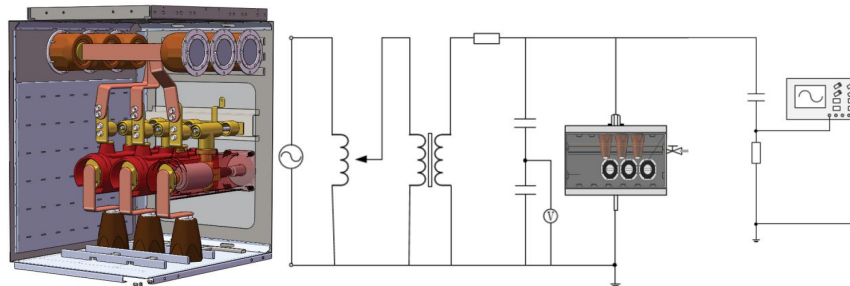


Figure 3. Modeling of switchgear chamber and partial discharge experimental platform.

## 2. ANALYSIS OF HIGH VOLTAGE WINDING WAVE PROCESS IN C5F10O GAS DECOMPOSITION PROCESS

The various parameters in actual C5F10O gas insulated switchgear are distributed parameters, but in practical analysis, the centralized parameter chain network is usually used instead of actual distributed parameters to construct equivalent circuit of winding under impulse voltage. Due to the high frequency of impulse voltage and the small ratio of winding resistance to inductive and capacitive reactance, the damping effect of resistance can be ignored in analysis. Therefore, equivalent circuit network is only composed of inductance and capacitance. The accuracy of calculating the equivalent parameters of inductance and capacitance in the equivalent circuit network has a significant impact on the calculation results of the wave process[9]. To ensure the accuracy of the analysis results of the winding wave process, it is necessary to first calculate inductance and capacitance parameters according to actual structure of transformer winding in Figure 4.

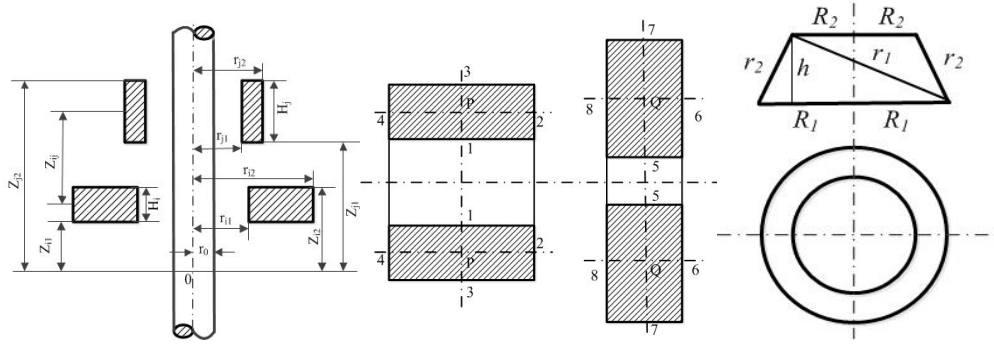


Figure 4. Layout diagram of coaxial line cake mutual inductance calculation number.

The calculation of the inductance component affected by C5F10O gas insulated iron core can be performed using the following formula:

$$M_{ij1} = 2\mu_0 w_i w_j \int_0^\infty b_3(p) F(p) dp \quad (1)$$

$$b_3(p) = \frac{(1-\nu)I_0(pr_0)I_1(pr_0)pr_0}{(1-\nu)K_0(pr_0)K_1(pr_0)pr_0 + \nu} \quad (2)$$

$$F(p) = \frac{4}{S_i S_j p^6} \sin \frac{pH_j}{2} \sin \frac{pH_i}{2} \cos pd_{ij} \int_{pr_1}^{pr_2} xK_0(x) dx \int_{pr_1}^{pr_2} xK_1(x) dx \quad (3)$$

$I_0$ ,  $I_1$ ,  $K_0$ ,  $K_1$  is first and second types of zero order and first-order modified Bessel functions. Therefore, referring to the calculation experience of actual C5F10O gas insulated switchgear, when upper limit of integration is set, sufficient calculation accuracy can already be guaranteed. For the integral of the equation, if the modified Bessel function in the equation is expanded into the infinite series, the calculation will become very cumbersome. In practical calculations, the asymptotic formula of the modified Bessel function can be introduced to replace the series of slowly converging Bessel functions. This article only takes first type of zero order modified Bessel function as example to provide corresponding asymptotic formula (where  $t=x/3.75$ ).

$$I_0(x) = 1 + 3.5156229t^2 + 3.0899424t^4 + 1.2067492t^6 + 0.2659732t^8 + 0.0360768t^{10} + 0.0045813t^{12} + \varepsilon \quad (4)$$

$$x^{0.5} e^{-x} I_0(x) = 0.39894228 + 0.01328592t^{-1} + 0.00225319t^{-2} - 0.0015756t^{-3} + 0.00916281t^{-4} - 0.02057706t^{-5} + 0.02635537t^{-6} - 0.01647633t^{-7} + 0.00392377t^{-8} + \varepsilon \quad (5)$$

Then  $\rho \leq 0.5$ :

$$\psi = 4\pi \left[ \left( 1 + \frac{\rho^2}{24} + \frac{11}{2880}\rho^4 + \dots \right) \ln \frac{4}{\rho} - \frac{1}{2} + \frac{43}{288}\rho^2 + \frac{1}{150}\rho^4 + \dots \right] \quad (6)$$

Then  $\rho > 0.5$ :

$$\Delta = \frac{\mu_0}{2} w^2 d \left[ \frac{\pi}{3\gamma} \left( 1 + \frac{\alpha^2}{5} + \frac{\alpha^2 \gamma^2}{15} - \frac{2}{35} \alpha^4 \right) - \left( \frac{\alpha^2}{8} - \frac{\alpha^4}{64} + \frac{7}{384} \alpha^2 \rho^2 \right) \ln \frac{4}{\rho} \right. \\ \left. - \frac{1}{6\gamma^2} \left( 1 + \frac{\alpha^2}{4} + \frac{\alpha^2 \rho^2}{4} \right) \ln \gamma - \frac{\alpha^2}{8} - \frac{25}{72} \frac{1}{\gamma^2} + \frac{\alpha^2 \rho^2}{2304} - \frac{1}{180\gamma^4} - \frac{23}{288} \frac{\alpha^2}{\gamma^2} - \frac{31\alpha^4}{2304} \right] \quad (7)$$

From the characteristics of the potential distribution of the flower arrangement tangled wire cake, it can be seen that the more parallel wires there are in the wire cake, the larger the equivalent capacitance, but the more welding turns need to be carried out, and the more time required for winding. This has led to the increasingly widespread application of flower arrangement tangled wire cakes in high-voltage winding of C5F100 gas insulated switchgear[10].

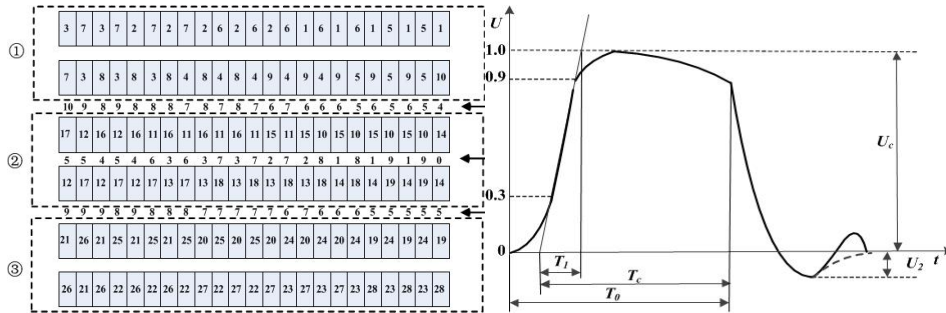


Figure 5. Potential distribution of the second double cake oil passage of C5F100 gas.

### 3. THERMAL DECOMPOSITION CHARACTERISTICS OF C5F100 GAS UNDER LOCAL OVERHEATING FAULT IN GIS

The existing research has confirmed the possibility of using environmentally friendly insulation gases to replace SF6 in medium and low voltage switchgear. Through the improvement of insulation structure, the practical application cases of nitrogen and dry air mixed gas insulation have appeared in the switchgear below 35kV. However, in order to promote it at higher voltage levels and ensure the size and footprint of the original switchgear[11], it is necessary to overcome the problem of insufficient insulation performance of type of gas and use environmentally friendly gas C5F100 with better performance. Structure is designed based on the E-field characteristics of C5F100 and its mixed gas shown in Figure 6.



Figure 6. Local overheating caused by poor contact, current overload, etc.

Determine the optimal mixing ratio of C5F100/and air, and obtain accurate electrical strength data. Based on this, determine the allowable field strength, and then carry out the selection of the insulation materials and insulation structure design for key positions such as through wall sleeves in switchgear, isolation and grounding fractures of three position isolating switches, and supporting insulators to match the insulation strength of C5F100/air mixed gas shown in Figure 7.

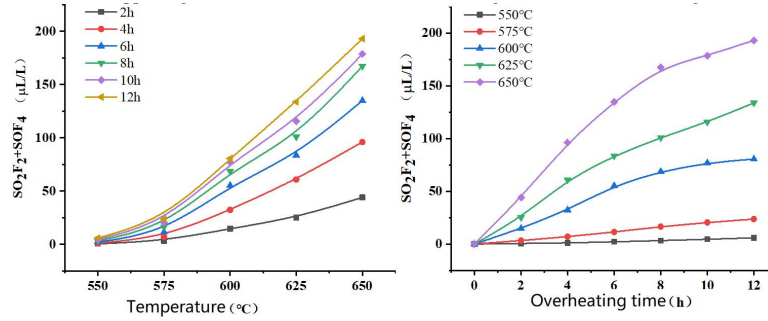


Figure 7. SO<sub>2</sub>F<sub>2</sub>+SOF<sub>4</sub> content and fault temperature.

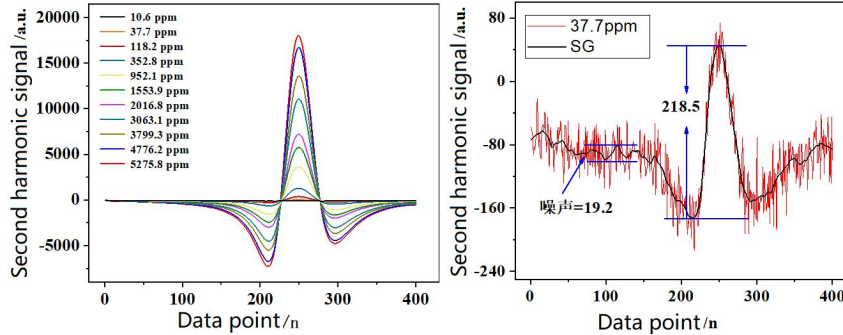


Figure 8. Second harmonic signal of 37.7 ppm HF gas.

The sensing system for H<sub>2</sub>O and HF gas detection was designed using 1392nm and 1278nm DFB lasers combined with absorption spectroscopy technology. Gas adsorption experiments were conducted on optical gas absorption cells made of four different materials, SUS304, 6061 aluminum alloy, PTFE, and PVDF. The analysis of the experimental results showed that there were differences in adsorption saturation time among the optical gas absorption cells made of different materials, but it did not affect the accuracy of the measurement results. Among them, the PVDF gas cell had the shortest response time and the best performance after adsorption saturation shown in Figure 8. Although there are differences in response time between coating materials, the differences are not significant. Therefore, in practical applications, the adsorption of H<sub>2</sub>O and HF gases by the pool material can be ignored[12,13].

Based on the theory of laser light transmission, in-depth research and analysis were conducted on the theory of long path multiple reflection gas absorption cells used in TDLAS systems. The Herriott type multiple reflection gas absorption cell was simulated and designed using TracePro ray tracing software, and the design parameters for achieving high stability multiple reflection the long path gas cells were obtained. The theoretical and simulation research on gas pools provides important parameter guarantees for the development of the device[14].

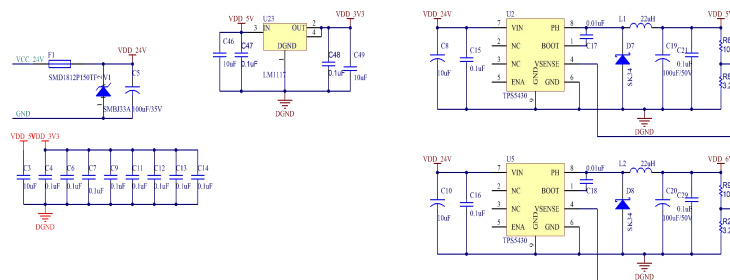


Figure 9. Power supply schematic diagram.

The display host LCD circuit is powered by the 5V power supply, while the general digital circuit is powered by a 3.3V power supply. This system uses the TPS5430 DC-DC buck chip to reduce the voltage to 5V, and then uses the LDO chip LM1117-3.3 to reduce the voltage to 3.3V for use in digital system. Most sensing systems initially use the 12V~24V DC power supply for direct power supply, but there is no pre voltage reduction circuit inside the sensing unit. The separate LDO is set up inside to reduce the voltage to 5V. If the 24V or 12V is used to directly supply power to it, on the one hand, the power supply efficiency is low, and on the other hand, the power supply system heats up severely. Therefore, a

separate voltage reduction circuit is set up to reduce the voltage to 6V, which is used separately for the sensor unit. The schematic diagram of the power supply is shown in the following Figure 9.

#### 4. APPLICATION OF DIGITAL PHASE-LOCKED TECHNOLOGY TO EXTRACT THE SECOND HARMONIC OF C5F10O GAS COMPONENTS

Selecting liquid crystal as the LED backlight, the structure consists of multiple LEDs connected in series and requires constant current boost driving. The project team selected MP3202 as the main chip to implement LCD backlight driving, as shown in the schematic diagram shown in Figure 10.

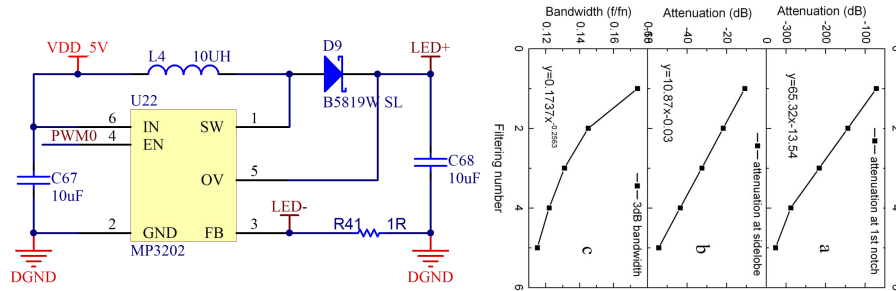


Figure 10. The relationship between attenuation characteristics and order of SG filter.

The out of band attenuation of SG smoothing filter is only 8-12 dB. When larger out of band attenuation is required, SG filter can be reused for data. Figure 10 shows the amplitude frequency characteristics of repeatedly using SG (7,2) filters. The multi lobe structure remains unchanged, and the starting frequency of the stopband remains unchanged. However, the amplitude of the lobes affects the cutoff frequency  $f_c$ , out of band attenuation ratio, and stopband attenuation ratio. Fit the relationship between the frequency characteristics and repetition times of the SG filter. Every time SG filtering is performed, the amplitude of the first stopband decreases by about 65dB. The amplitude of the first sidelobe decreases by about 10.8dB, and the -3dB bandwidth decreases accordingly, following a negative exponential law shown in Figure 11.

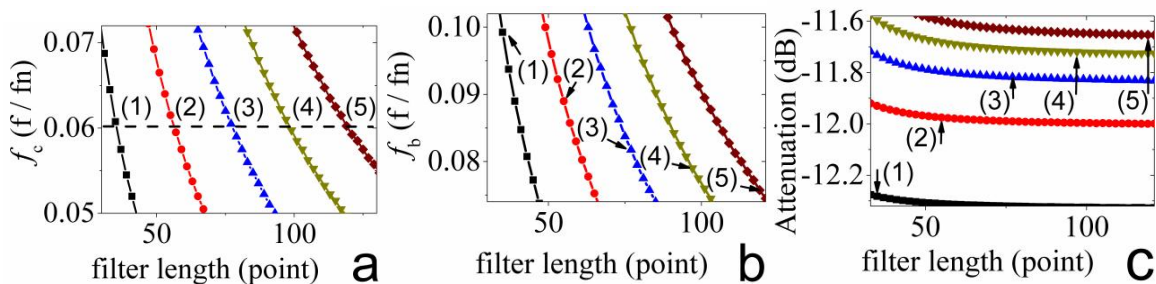


Figure 11. Selection of SG filter parameters.

Firstly, based on the insulation characteristics of C5F10O/air mixture gas, select suitable solid insulation materials (such as epoxy resin, polytetrafluoroethylene, etc.) and appropriate allowable field strength, and design an insulation structure suitable for the C5F10O/air mixture gas. Secondly, based on the designed insulation structure, numerical modeling and simulation are used to analyze the electric field distribution of the insulation structure inside the gas chamber. Combined with on-site testing, typical insulation structure power frequency, partial discharge, and impulse flash-over characteristics are tested. Based on experimental data, the insulation structure is further optimized, and finally the internal insulation structure of the switchgear with C5F10O/air mixed gas as main insulation medium is proposed. Environmentally friendly 35kV fully enclosed metal switchgear with C5F10O/air mixed gas as the insulation medium will be trial produced, and self inspection will be carried out according to the type tests specified in national or industry standards. The assembly process and layout of the final switch will be optimized, and purpose of obtaining third-party test reports after inspection will be achieved, completing the production of the prototype.

#### 5. CONCLUSION

Referring to the calculation experience of actual C5F10O gas insulated switchgear, when upper limit of integration is set, sufficient calculation accuracy can already be guaranteed. For the integral of the equation, if the modified Bessel function in the equation is expanded into the infinite series, the calculation will become very cumbersome. In practical

calculations, the asymptotic formula of the modified Bessel function can be introduced to replace the series of slowly the converging Bessel functions. This article takes first type of zero order modified Bessel function as example to provide corresponding asymptotic formula (where  $t = x/3.75$ ).

The display host LCD circuit is powered by the 5V power supply, while the general digital circuit is powered by a 3.3V power supply. This system uses the TPS5430 DC-DC buck chip to reduce the voltage to 5V, and then uses the LDO chip LM1117-3.3 to reduce the voltage to 3.3V for use in digital system. Most sensing systems initially use the 12V~24V DC power supply for direct power supply, but there is no pre voltage reduction circuit inside the sensing unit. The separate LDO is set up inside to reduce the voltage to 5V.

## ACKNOWLEDGMENTS

This article is sponsored by the Chongqing Electric Power Company's technology project (52202323000C).

## REFERENCES

- [1] Ho SI, Yang S, Ni G, et al. An improved PSO method with application to multimodal functions of inverse problems[J]. IEEE transactions on Magnetics, 2007, 43(4): 1597-1600.
- [2] Coelho L, Ayala HVH, Alotto P. A multiobjective Gaussian particle swarm approach applied to electromagnetic optimization[J]. IEEE Transactions on Magnetics, 2010, 46(8): 3289-3292.
- [3] Liu X, Wang S, Qiu J, et al. Robust optimization in HTS cable based on design for Six Sigma[J]. IEEE Transactions on Magnetics, 2008, 44(6): 978-981.
- [4] B. Chervy, H. Riad and A. Gleizes, "Calculation of the interruption capability of SF6/CF4 and SF6/C2F6 mixtures. I. Plasma properties," in IEEE Transactions on Plasma Science, vol. 24, no. 1, pp. 198-209, Feb. 1996, doi: 10.1109/27.491760.
- [5] Larin, Alexander & Meurice, N. & Trubnikov, Dmitrii & Vercauteren, Daniel. (2004). Theoretical analysis of the synergism in the dielectric strength for SF6/CF4 mixtures. Journal of Applied Physics. 96. 109-117. 10.1063/1.1751637.
- [6] Li X, Zhao H, Jia S, et al. Study of the dielectric breakdown properties of hot SF6-CF4 mixtures at 0.01-1.6 MPa[J]. Journal of Applied Physics, 2013, 114(5):053302.1-053302.7.
- [7] Raj P-D-V, Kumar SS, Raja J, et al. Particle swarm optimization based energy optimized dynamic voltage restorer[C]. International Conference on Power System Technology, New Delhi, 2008: 1-6.
- [8] Zhang, Boya & Zhang, Ziyue & Xiong, Jiayu & Yang, Tao & Li, Xingwen & Chen, Li & Li, Chenwei & Deng, Yunkun. (2020). Thermal and Electrical Decomposition Products of C5F10O and Their Compatibility with Cu (111) and Al (111) surfaces. Applied Surface Science. 145882. 10.1016/j.apsusc.2020.145882.
- [9] Li, Yi & Zhang, Xiaoxing & Xiao, Song & Chen, Dachang & Chen, Qi & Wang, Dibo. (2018). Theoretical evaluation of the interaction between C5-PFK molecule and Cu (1 1 1). Journal of Fluorine Chemistry. 208. 10.1016/j.jfluchem.2018.01.005.
- [10] Zhang, Xiaoxing & Li, Yi & Xiao, Song & Tang, Ju & Tian, Shuangshuang & Deng, Zaitao. (2017). Decomposition Mechanism of C5F10O: An Environmentally Friendly Insulation Medium. Environmental Science & Technology. 51. 10.1021/acs.est.7b02419.
- [11] Li, Yi & Zhang, Xiaoxing & Xiao, Song & Chen, Qi & Wang, Dibo. (2018). Decomposition characteristics of C5F10O/air mixture as substitutes for SF6 to reduce global warming. Journal of Fluorine Chemistry. 208. 10.1016/j.jfluchem.2018.01.015.
- [12] Rokunohe, Toshiaki & Yagihashi, Yoshitaka & Endo, Fumihito & Oomori, Takashi. (2005). Fundamental insulation characteristics of air; N2, CO2, N2/O2, and SF6/N2 mixed gases. Electrical Engineering in Japan. 155. 9 - 17. 10.1002/eej.20348.
- [13] Wada J, Ueta G, Okabe S. Evaluation of breakdown characteristics of N2 gas for non-standard lightning impulse waveforms under non-uniform electric field- breakdown characteristics for single-frequency oscillation waveforms -[J]. IEEE Transactions on Dielectrics & Electrical Insulation, 2012, 19(1):263-273.
- [14] J. Wada, G. Ueta and S. Okabe, "Evaluation of breakdown characteristics of N2 gas for non-standard lightning impulse waveforms under non-uniform electric field --breakdown characteristics for single-frequency oscillation waveforms -," in IEEE Transactions on Dielectrics and Electrical Insulation, vol. 19, no. 1, pp. 263-273, February 2012, doi: 10.1109/TDEI.2012.6148527.